

Spatial discrete element analysis of problem on floor buckling in underground openings

SV Klishin* and AF Revuzhenko**

Chinakal Institute of Mining, Siberian Branch, Russian Academy of Science,
Novosibirsk, Russia

E-mail: *sv.klishin@gmail.com, **revuzhenko@yandex.ru

Abstract. The authors analyze 3D problem on instability of a long arch cross-section opening using the method of discrete elements. Under analysis is loading by gravitational and tectonic stresses. Dilatancy, dry friction and viscosity are taken into account. It is assumed that contacting particles have an in-between elastic bonding element that fails under critical load. The article presents kinematic patterns of deformation and failure of surrounding rock mass around an underground opening.

1. Introduction

Buckling is one of the most widely spread processes induced by overburden pressure. Investigation of different types of buckling, review of the current knowledge on buckling mechanism and elaboration of measures aimed to predict and prevent such events is an important task, both theoretically and practically.

Consider a boundary value problem. Let an arch cross-section opening be driven in a rock mass at a depth H from free surface (Figure 1). The task is to define stress state of surrounding rock mass and the nature of buckling in the floor of the opening.

The in situ researches undertaken by different scientists show that buckling takes place in floor rocks when they are weaker than rocks in sidewalls and roofs of underground excavations. The explanation of the reason for the deformation reads that stronger rocks underlaid by weaker rocks act as a block die and deform considerably less as compared with the weaker underlying rocks.

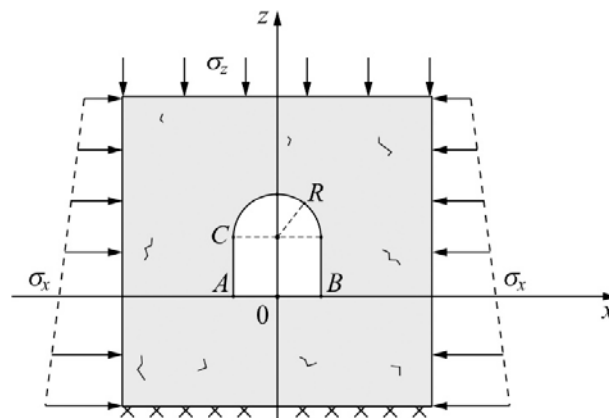


Figure 1. Schematic representation of the problem on floor buckling in underground opening.

The theoretical approaches to this problem can conventionally be divided into two groups. The first group are engineering solutions based on the hypothesis of a rigid block die [1–3]. These solutions use theories of limiting state and mostly consider deformation only of a part of rock mass (floor or roof). The material constraint of this approach is disregard of the rock mass loading history before limiting state. The second group rest upon the theory of elasticity and plasticity. The scope of stress state analysis in this case covers entire rock mass surrounding an underground opening [4–8]. Since displacements are small in elastic or elastoplastic formulations, the inference on buckling is based on the assumption of the floor rock loosening in the zone of rock crushing and on the analysis of strain field resultant from a boundary value problem solution.

The concept of rock mass as a medium with inner sources and sinks of energy backs the two-dimensional mathematical model constructed in [9, 10], considering internal block structure of rock mass, anisotropy of properties and sliding at block interfaces with regard to strength loss. The model is used to analyze numerically a problem on deformation of heavy rock mass surrounding a long horizontal opening with an arch cross-section. It is shown that zones of weakening and residual strength develop successively both in sidewalls and in floor and, finally, embrace the whole perimeter of the opening. The process of deformation is accompanied by uncontrollable dynamic release of elastic energy accumulated in the rock mass.

Evidently, the continuum formulations based on the methods of the elasticity and plasticity theory need no hypothesizing on limiting states. At the same time, it is required to construct closed systems of equations. At present, generally acknowledged equations of deformation of a medium remain yet to be developed.

Under such circumstances, it seems relevant to select an approach based on the discrete element method (DEM). This method allows determining evolution of stress state in rock mass both at the pre-limiting stage and at the stage of transition to localization of shearing and failure. The method is advantageous for needing no hypotheses on limiting state and no continuum equations to be postulated.

Originally, DEM was applied to solution of rock mechanics problems [15]. Now the method enjoys wide popularity in solving many problems in geomechanics [16, 17]. The essence of the method is replacement of a real medium by a packing of particles with introduction of laws of the particle interaction. The shape of the particles is a free parameter to be selected based on specific considerations. Mostly, it is assumed that the discrete elements have spherical form with the preset radii. This method induces no additional difficulties in solving problems with high (finite) values of strains and rotations. Thus, this method is a fundamental alternative to classical methods based on conventional knowledge on the continuum mechanics.

2. Discrete element method

According to DEM, a particulate material is represented by a set of N spherical particles (discrete elements). Each i -th element has a radius r_i and possesses the known physical properties: density, elastic and viscous moduli, friction, cohesion, etc. ($i=1, \dots, N$). Movement of a discrete element includes translational and rotational motions, and is given by

$$m_i \ddot{\mathbf{x}}_i = \sum_j \mathbf{f}_{ij} + m_i \mathbf{g}, \quad (1)$$

$$I_i \ddot{\boldsymbol{\theta}}_i = \sum_j (\mathbf{r}_{ic} \times \mathbf{f}_{ij} + \mathbf{M}_{r,ij}). \quad (2)$$

Here, points mean differentiation with respect to time t ; \mathbf{x}_i is the radius-vector of the center of gravity of an i -th particle; $\boldsymbol{\theta}_i$ is the rotation of an i -th particle relative to the coordinate axes; m_i is the mass; I_i is the moment of inertia; \mathbf{g} is the gravitational acceleration; \mathbf{r}_{ic} is the vector directed from the center of an i -th particle to the point of contact; the force \mathbf{f}_{ij} acts on an i -th particle from the side of a j -th particle and depends on the overlap of the particles and on the elastic and viscous moduli; $\mathbf{M}_{r,ij}$ is the moment of rolling resistance between particles or along the domain boundary. Summing in (1) and (2)

involves all elements and boundaries that contact the current i -th particle. The shape of discrete elements is assumed unaltered for the period of contact; therefore, the degree of deformation of the elements is characterized by the value of overlap of contacting particles.

With the data on the law of motion and contact interaction between particles (equations (1) and (2)), as well as with the initial and boundary conditions, it is possible to construct solutions of the equations and to define evolution of stress state of a medium.

The program support designed based on DEM at the Institute of Mining, SB RAS enables numerical consideration of different modes of motion in a granular material composed of individual spherical particles [18, 19].

Below an illustration is given of the capacities of this method in the analysis of stress state in rocks and particulate media. Let a material specimen be composed of individual discrete particles (Figure 2a). The particles have the parameters: density $\rho_i = 2500 \text{ kg/m}^3$, elasticity modulus $E_i = 3 \text{ GPa}$, Poisson's ratio $\nu_i = 0.25$, external friction angle $\varphi_{ij} = 25^\circ$, the diameters of the particles are selected from the uniform distribution over the interval from 0.0015 to 0.0025 m. The boundaries of domain of the specimen are perfectly smooth, the force of gravity is absent. Loading is implemented as uniform compression at a constant pressure $P = 10^4 \text{ Pa}$ and with a later on increase in σ_z oriented in parallel to the vertical axis towards the material. The overall deformation ε_z upon completion of loading was 0.3. Figures 2b and 2c show the plots of the relative stress σ_z / P and the relative volume V_r depending on the density of the initial packing. The curve 1 illustrates a dense packing, the curve 2 characterizes a loose packing. Obviously, it is possible to obtain materials with different strength properties by simply and only changing the initial density of specimens. The resultant consistent patterns are confirmed by in situ measurements and laboratory experiments [20].

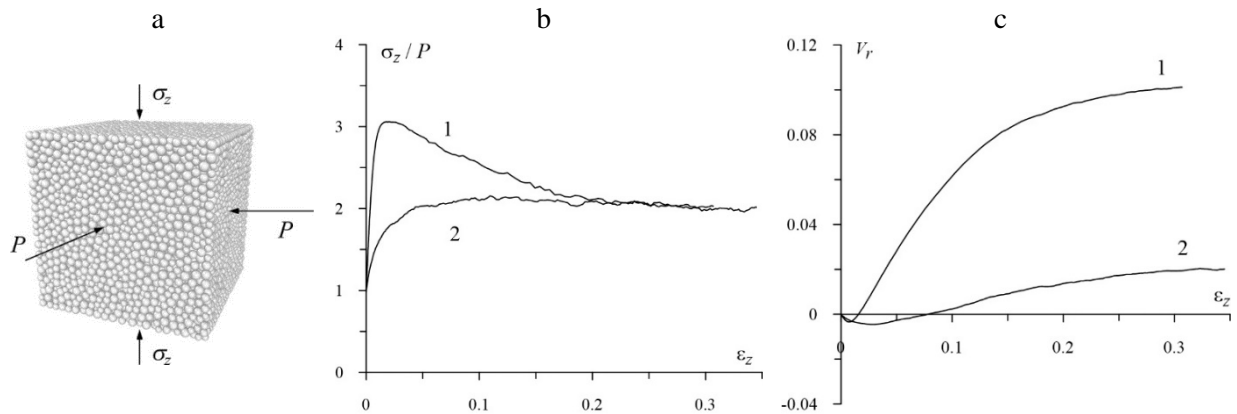


Figure 2. (a) The numerical experiment on triaxial compression of a particulate material; (b) stress–strain relationship in the tests; (c) change in specimen volume under compression: 1—dense packing; 2—loose packing.

A rock is a cohesive material; for this reason, the described model of particulate material deformation needs introduction of an additional bonding element (cohesion) between contacting particles. With this end in view, we use the procedure from [21–23].

The increments in the forces and moments induced in the bonding element by the particle interaction are given by

$$\begin{aligned} \Delta \hat{F}_n &= -\hat{k}_n A \Delta u_n, \quad \Delta \hat{F}_t = -\hat{k}_t A \Delta u_t, \\ \Delta \hat{M}_n &= -\hat{k}_t J \Delta \theta_n, \quad \Delta \hat{M}_t = -\hat{k}_n I \Delta \theta_t, \end{aligned} \quad (3)$$

where A is the intersection area between a particle and the bonding element; I and J are the inertia moment and the polar moment of inertia of the bonding element, respectively (Figure 3); Δu_n , Δu_t , $\Delta \theta_n$ and $\Delta \theta_t$ are the increments in the components of velocities and angular velocities in the normal and tangential directions, respectively.

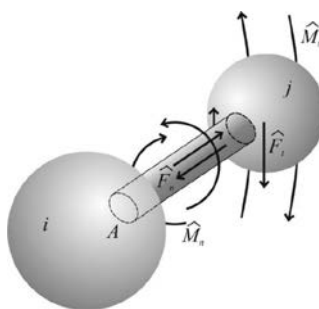


Figure 3. Schematics to find actual forces in bonding element.

The maximum tension force and shear force caused in the bonding element by relative motion of particles are

$$\begin{aligned}\hat{\sigma}_{\max} &= -\frac{\hat{F}_n}{A} + \frac{|\hat{M}_t| \hat{R}}{I}, \\ \hat{\tau}_{\max} &= -\frac{|\hat{F}_t|}{A} + \frac{|\hat{M}_n| \hat{R}}{J},\end{aligned}\quad (4)$$

where $\hat{R} = \min(r_i, r_j)$. When the maximum tension force in the bonding element exceeds the tension bond strength ($\hat{\sigma}_{\max} > \sigma_c$), or the maximum shear force is higher than the shear bond strength ($\hat{\tau}_{\max} > \tau_c$) of the material, the bonding element fails and henceforth the particles are only subjected to the forces described by the equations (1) and (2).

By way of illustration, Figure 4 depicts a numerical experiment on destruction of a cylindrical specimen simulating a rock core composed of individual particles with cohesion under compression. It is seen in Fig. 4b that the load distribution line contains both elastic strain branch, and branches of weakening and residual strength typical of destruction processes in real materials.

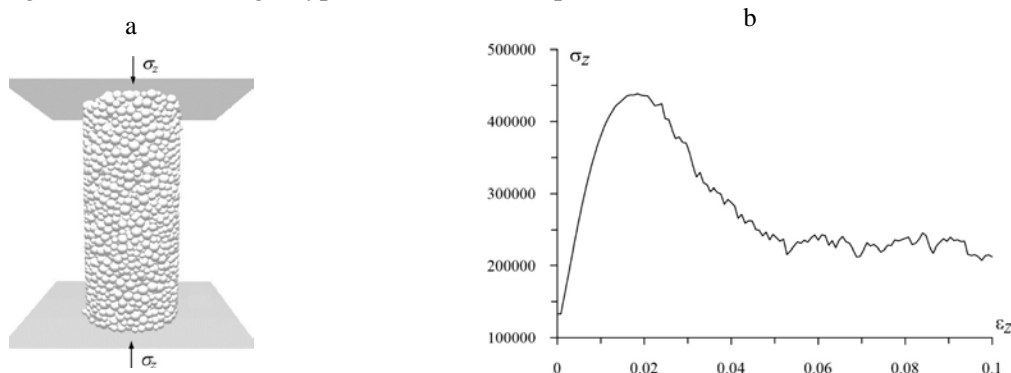


Figure 4. Uniaxial compression of rock specimen—numerical experiment: (a) schematic of the experiment; (b) stress–average strain curve.

In this way, by introduction of cohesion between discrete elements constituting a particulate material, it is possible to describe deformation and failure processes in cohesive rocks. Now we address again the problem on floor buckling in an underground opening. Figure 5 demonstrates the schematic of 3D numerical experiment. The experimental domain is represented by $N = 92000$ discrete elements with the radii selected from a uniform distribution over the interval from 0.05 to 0.15 m.

In the problem under discussion, the opening has a width of 3 m and a height of 3.5 m; the size of the domain in the Oy axis direction is 2 m. The physical parameters of the particles are: density $\rho_i = 2500 \text{ kg/m}^3$, elasticity modulus $E_i = 8 \text{ GPa}$; Poisson's ratio $\nu_i = 0.25$ and external contact friction angle $\varphi_{ij} = 28^\circ$. The stiffness coefficients of the particle bonding in the normal and tangential directions: $\hat{k}_n = \hat{k}_t = 10 \text{ MPa}$; the critical bonding strengths: $\sigma_c = 8 \text{ MPa}$ and $\tau_c = 5 \text{ MPa}$. The

boundaries of the domain are rigid and perfectly smooth walls. The gravitational vector is oriented vertically downward and its magnitude is 9.81 m/s^2 . The lower boundary is assumed fixed.

The loading process involves two methods. The first method is moving the upper boundary at a constant low velocity $u_z = \text{const}$ in the direction of the opening, with the left-hand and right-hand boundaries being fixed. The second method is shifting the left- and right-hand boundaries at a velocity $u_x = \text{const}$ in the direction of the opening, with the upper boundary being fixed.

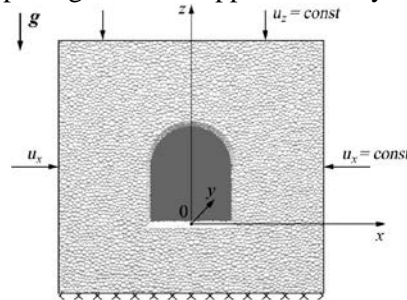


Figure 5. Numerical experiment on deformation of rock mass with a weakening in the form of an arch cross-section opening.

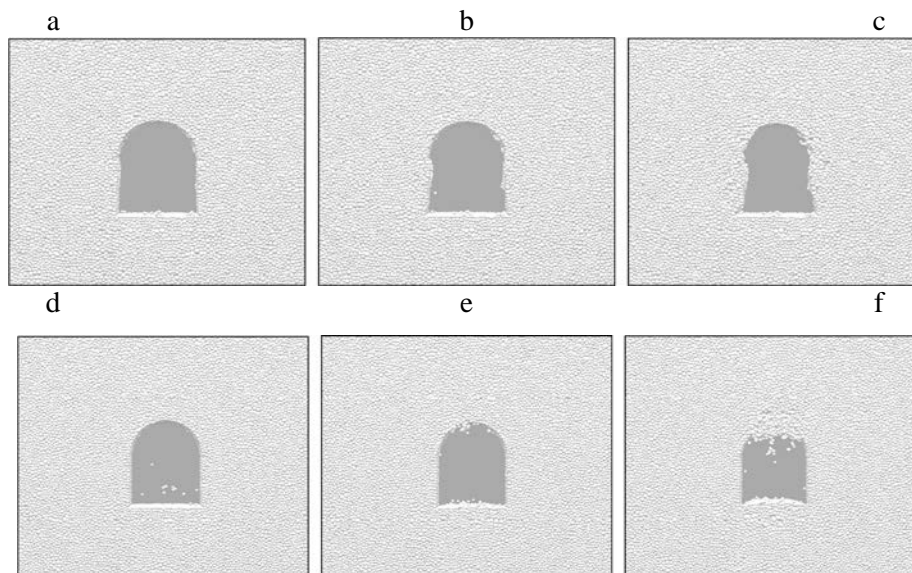


Figure 6. Deformation of surrounding rock mass around an opening at fixed moments of time: (a)–(c) action of gravitational stresses; (d)–(f) action of tectonic stresses.

The numerical experiment has discovered essential dependence of the opening perimeter deformation on the rock mass deformation history as a function of deformation method. When it is assumed that gravitational (vertical) stresses prevail, the opening sidewalls deform as Figure 7a–7c show. For dominating tectonic (horizontal) stresses, the failure pattern is shown in Figures 7d–7f where the instability and failure occur in the roof and floor of the opening.

3. Conclusion

To analyze buckling of floor rocks in mines, it seems most relevant to use the discrete element method. Under prevailing gravitational (vertical) stresses, failure takes places in the sidewalls of underground openings. Under dominating tectonic (horizontal) stresses, instability and failure occur in the floor and roof of the openings.

4. Acknowledgements

The investigation was done under support of Russian Science Foundation, project № 16-17-10121

References

- [1] Tsimbarevich PM 1948 *Rock Mechanics* Moscow: Ugletekhizdat (in Russian)
- [2] Chernyak IL 1978 *Prevention of Floor Buckling in Underground Excavations* Moscow: Nedra
- [3] Sokolovsky VV 1960 *Statics of Granular Medium* Moscow: Fizmatlit (in Russian)
- [4] Kovalenko VV and Ryazantsev AP 2013 *Evaluation of Process Variables for Prevention of Floor Rock Buckling in Coal Mines* Dnepropetrovsk: Nats. Gorn. Univ. (in Russian)
- [5] Voloshin VA, Rib SV, Fryanov VN and Cherepov AA 2015 Formation of increased overburden pressure zones under influence of coal pillar-block die in bed series mining *GIAB* No 7 pp. 23–29
- [6] Khomyakova A.A., Nikitina A.M., Rib S.V., Borzykh D.M. Analysis of influence exerted by a diminishing coal pillar on floor rock buckling in a roadway. In: *High Technologies of Mineral Mining and Utilization: Collection of Papers*. V.N. Fryanov (Ed.). Novokuznetsk: Sib. Gos. Industr. Univ., 2014, pp. 118–123. (in Russian)
- [7] Demin VF, Yavorsky VV, Demina TV and Steflyuk YuYu 2015 Efficient methods to prevent floor rock buckling in gateways in coal mines *Usp. Sovr. Est. Nauk* No 12 pp. 95–99
- [8] Kuzmin SV and Salvasser IA 2014 Factors and classification criteria of buckling *Byull. KuzGTU* No 3(103) pp. 43–44
- [9] Lavrikov SV, Mikenina OA, Revuzhenko AF and Shemyakin EI 2008 The concept on non-Archimedean multiscale space and models of plastic media with structure *Physical Mesomechanics* Vol 11 N 3 pp. 233–246
- [10] Lavrikov SV 2010 Calculation of stress state in weakening block rock mass around an opening *Physical Mesomechanics* Vol. 13 No 4 pp. 53–63
- [11] Labuz Joseph F and Zang A 2012 Mohr–Coulomb failure criterion *Rock Mechanics and Rock Engineering* Vol. 45 No 6 pp. 975–979
- [12] Abbo AJ and Sloan SW 1995 A smooth hyperbolic approximation to the Mohr-Coulomb yield criterion *Computers and Structures* Vol. 54 No 3 pp. 427–441
- [13] Hoek E and Brown ET Empirical strength criterion for rock masses *J. Geotech. Engng. Div., ASCE 106(GT9)* pp. 1013–1035
- [14] Hoek E 1983 Strength of jointed rock masses *Géotechnique* Vol 23 No 3 pp. 187–223
- [15] Cundall PA and Strack ODL 1979 A distinct element model for granular assemblies *Géotechnique* Vol 29 No 1 pp. 47–65
- [16] Klishin SV, Klishin VI and Opruk GYu 2013 Modeling coal discharge in mechanized thick and steep oal mining *Journal of Mining Science* Vol 49 No 6 pp. 932–940
- [17] Lavrikov SV and Revuzhenko AF 2015 DEM code-based modeling of energy accumulation and release in structurally heterogeneous rock masses *AIP Conference Proceedings 1683*
- [18] Klishin SV and Revuzhenko AF 2014 3D discrete element approach to Janssen’s problem *Journal of Mining Science* Vol 50 No 3 pp. 417–422
- [19] Klishin SV and Revuzhenko AF 2015 A class of vortex flows in granular medium *Journal of Mining Science* Vol 51 No 6 pp. 1070–1076
- [20] Bishop AW 1972 Shear strength parameters for undisturbed and remoulded soil specimens *Stress–Strain Behavior of Soils: Proceedings of the Roscoe Memorial Symposium* Parry RHG (Ed) Cambridge University pp. 3–58.
- [21] Potyondy DO and Cundall PA 2004 A bonded-particle model for rock *International Journal of Rock Mechanics and Mining Sciences* Vol 41 No 8 pp. 1329–1364
- [22] Mohammad Sadegh Asadi, Vamegh Rasouli and Giovanni Barla 2012 A bonded particle model simulation of shear strength and asperity degradation for rough rock fractures *Rock Mechanics and Rock Engineering* Vol 45 no 5 pp. 649–675
- [23] Obermayr M, Dressler K, Vrettos C and Eberhard P 2013 A bonded-particle model for cemented sand *Computers and Geotechniques* Vol 49 pp. 299–313